Experimental study of water-in-oil droplet micro-explosion using LIF measurements : effect of radiative heating configuration

Thomas Naudin, Dominique Tarlet, R Calabria, Patrizio Massoli, Jérôme Bellettre

ILASS-Americas 32nd Annual Conference on Liquid Atomization and Spray Systems, May 22-25, 2022

Experimental study of water-in-oil droplet micro-explosion using LIF measurements : effect of radiative heating configuration

T. Naudin[a], D. Tarlet[a], R. Calabria[b], P. Massoli[b], and J. Bellettre[a*]
[a]Laboratoire de Thermique et Energie de Nantes (LTeN)
Nantes University - CNRS UMR 6607
rue Christian Pauc, Nantes, France
[b]STEMS - CNR
Via Marconi, Napoli, Italy

Abstract

Water-in-oil (W/O) emulsions are innovative substitutes to the classical hydrocarbon fuels, because of the reduction of pollutant emissions allowed by the presence of water and, to the micro-explosion phenomenon. The micro-explosion is the fragmentation of a mother drop in a cloud of fine child droplets, due to the sudden vaporization of the water subdroplets within the emulsion drop. This is also called "secondary-atomization" and leads to a better fuel-air mixing, which increases combustion efficiency. Nevertheless, this phenomenon is stochastic, and can happen with greater or lesser efficiency. When the fragmentation of the emulsion drop is only partial, the event is called "puffing". The current objective of research in W/O emulsion atomization is to understand the way to optimize the micro-explosion occurrence and its efficiency. This paper presents the first results of the investigation of the behavior of W/O emulsions under radiative heating. The behavior of the dispersed water subdroplets during heating is investigated by means of Laser Induced Fluorescence (LIF) method, coupled to a fast camera. Natural convection motion of the water droplets is observed. Two emulsions of different mean diameter of the dispersed phase are tested which show a strong impact of coalescence on micro-explosion occurrence. Two heating schemes are presented and compared, namely radiative heating from the top and the bottom of the droplet.

*Corresponding Author:jerome.bellettre@univ-nantes.fr

Introduction

Water-in-Oil emulsions have been widely studied in the past decades, due to their capacity to reduce pollutants emissions while increasing combustion efficiency. The presence of water within the emulsion tends to lower the emission of different combustion products, such as carbon monoxide, thermal NOx and soot particles [1, 2, 3].

The other interest of W/O emulsions is the micro-explosion phenomenon (**FIGURE 1**). This event happens because of the difference of boiling temperature between the continuous oily phase and the water dispersed phase. This secondary atomization is the fragmentation of the so-called "mother drop" in a cloud of child droplets [4]. The micro-explosion results in a better fuel/air mixing, thus improving combustion efficiency.

The realization of the secondary atomization of a W/O emulsion droplet relies upon several factors that need to be controlled in order to obtain an optimal fragmentation. The size of the dispersed droplets is well-known as one of the dominant parameters to take into account in order to optimize micro-explosion rate [5]. Small-sized droplets results in a stable emulsion, while coarse emulsions will generate more coalescence, resulting in a significant secondary atomization [6, 7, 8]. The amount of surfactant needs to be controlled in order to have the right balance between stability and micro-explosion rate [9]. The non-complete breaking of the droplet also known as poor-atomization is called puffing [10, 11].
Moussa et al. [12] showed that micro-explosion rate increases when the dispersed water droplets are more prone to coalescence, which has been described with the adimensional Ohnesorge number. Additional studies showed that coalscence in W/O emulsion tends to increase micro-explosion occurrence probability and its quality [5, 13, 14].
The heating mode of the droplet, namely conductive, convective or radiative, results in different behaviors of the emulsion in term of micro-explosion delay and efficiency. The radiant heating presents the higher micro-explosion delay with respect to convective and conductive heating at a constant temperature, but also the most efficient disintegration (quantified by the number of child droplets measured [15]).

The radiant heating of emulsions or two-components droplets has still not been studied extensively. The difference in absorption of the incident radiant power between the two fluids constituing the emulsion is one of the key point to understand its behavior.
One of the innovative aspects of this work is the analysis of the motion (natural convection) of the dispersed water phase during the heating. The aim of this study is to understand if the internal convection happens in an emulsion droplet, and what is its impact on micro-explosion. The study of the motion of the dispersed phase is being made possible by Planar Laser-Induced Fluorescence (PLIF) technique. This method has been shown as promising for non-intrusive investigation in two-phase systems [16, 17, 18]. In the present study, micro-explosion occurrence is analyzed for two different emulsions dispersion size and two different heating schemes.

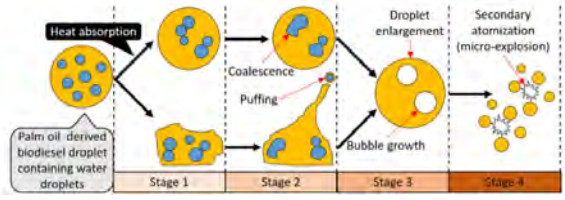

Figure 1. Mechanism of micro-explosion of W/O Droplet [19]

Experimental setup and procedure

Optical Setup

For this experiment, the Planar Laser Induced Fluorescence technique is used. This technique allows to observe the water droplets in an internal slide of the emulsion droplet. The experimental setup used is shown in **FIGURE 2**. The laser (Nd-YAG 2nd harmonic, Spectra Physics) emits a λ =532 nm beam. This beam is transformed in a laser sheet with a pair of cylindrical lenses. A Photron SA-X2 fast Camera is used for the frames recording. It allows a recording up to 12 500 frames per seconds at the maximum resolution of 2080x1024 pixels. In this work, the frame rate is varied between 500 and 2000 FPS since the interest is the behavior of the water subdroplets and not in the study of the micro-explosion itself, which mostly happens in a time less than 1ms [5].
The water droplets are tracked with Sodium salt Fluorescein (SIGMA-ALDRICH) with a concentration of 200 mg/L. This fluorescent tracer is highly soluble in water (up to 500 g/L) which allows to obtain a direct information on the size of the droplets. The fluorescein absorbs the incident laser beam at

λ=532 nm and emits the light at λ=550 nm. A pass-band filter (THORLABS-FB550) is coupled to the camera in order to keep only the re-emitted light.

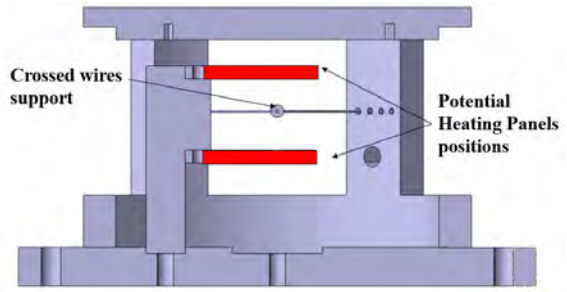

Figure 3. Droplet heating apparatus

Heating procedure

This work aims to investigate the impact of radiative heating on W/O atomization. The radiative heating system is composed of two radiative panels (BACH Resistors Ceramics GmbH) which can reach a maximum surface temperature of 750°C. The emissivity of the panels varies from 0.1 to 0.8 in the infrared band 3-12 µm. The temperature of the panels is controlled with a power supply, and a preliminary calibration of the temperature depending on the voltage applied is performed. The apparatus allows to mount the radiative panels in different positions, at the top, bottom and on the sides of the emulsion droplet. In the present study, only the bottom and top panel configurations are investigated (**FIGURE 3**). The distance of the panel to the center of the droplet in both configuration is fixed at 4 mm. The positioning of the panel has an important influence on the total heat flux supplied to the droplet. In the case of the heat source coming from the top, the droplet is heated mainly by radiative heat transfer and also by conduction, while for the heat source located at the bottom, the droplet is heated by radiation and also by convection. Our first approach was to calibrate the heating system in order to ensure the same total heat flux provided to the droplet in both top and bottom configurations. To this aim it was measured heating rate of pure n-Tetradecane droplet (D^2-Law) at different temperatures, until the same heating rate for both configurations was obtained. **FIGURE 4** shows D^2-Law for pure n-tetradecane droplet under top and bottom heating configurations at different panel temperatures. Curves of T_{panel} = 430°C in the bottom configuration and T_{panel}=700°C in the top configuration are the two which are overlapping, which corresponds to the same heat flux provided at the droplet.

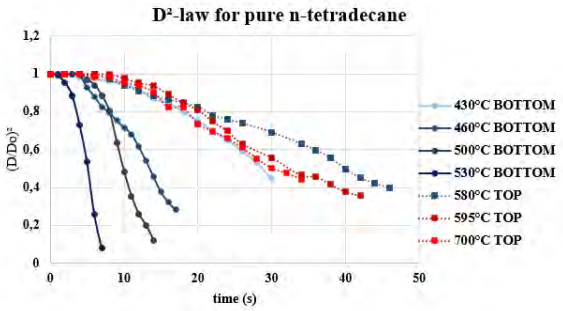

Figure 4. experimental D^2-law for pure n-tetradecane droplet

This method has for limitation the fact that optical properties of n-Tetradecane and water are completly different, so the radiative power absorbed is not the same in the case of an emulsion. However, it allows to have a starting point for the present investigation.

Emulsion Preparation

In order to investigate the coalescence rate of the water dispersed droplets and its impact on micro-explosion rate, two emulsions were prepared. Both are based on a continuous phase of n-tetradecane and had a composition of 7%$_m$ of water and 0.4%$_m$ of SPAN 83 surfactant. They were mixed using magnetic stirrer VMS-C4 (VWR). Mixing time and speed were varied in order to obtain two emulsions of respective mean diameter of 12 and 20 μm, which were measured with a Keyence VHX-7000 digital microscope. Each emulsion droplet was injected manually using a 5mL syringe, with a radius $R_d \approx 1$ mm.

Data post-treatment and Analysis

Raw images acquired were post-treated with MATLAB software (Image processing Toolbox) in order to obtain size and position of the water sub-droplets with time. Different operations such as contrast increasing, background subtraction, and watershed were operated. When errors are too important on droplets recognition, manual measurements were performed with the open source software Fiji.

Results and discussion

At the first stage of the experimental campaign, they were observed important differences concerning coalescence rate of emulsions, depending on both the dispersion in size of the water droplets and the loca-

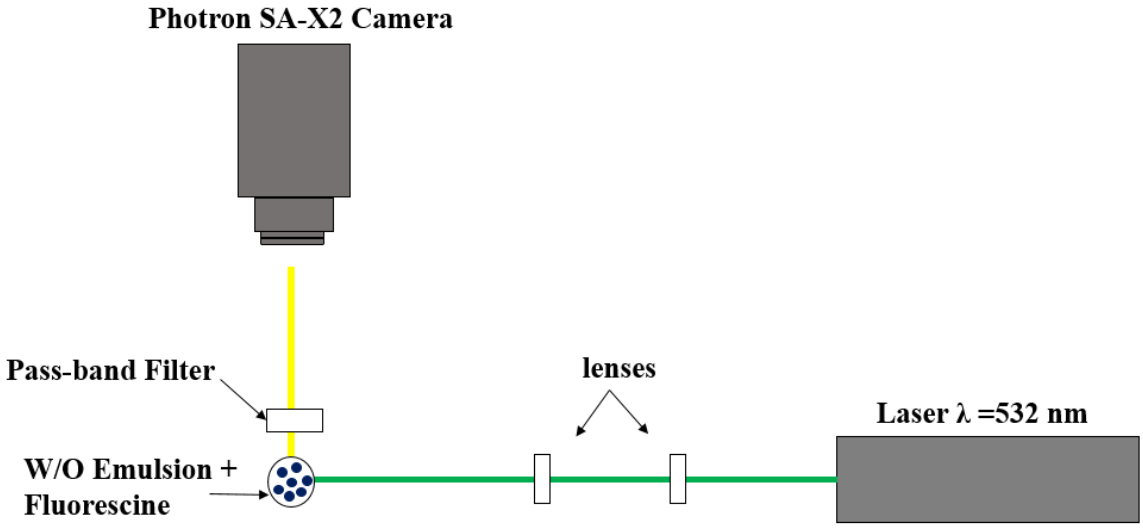

Figure 2. LIF experimental setup

tion of the heating source. Thus, the configurations reported in **Table 1** were studied:

Configuration	Water drop Mean Diameter (μm)	heating source location
A	20	Bottom
B	20	Top
C	12	Bottom
D	12	Top

Table 1. Configurations under study

Influence of emulsion dispersion on coalescence rate

The frames recorded during PLIF experiments were used to measure the evolution of the average water subdroplets for the 4 cases under study (coarse and fine emulsion, with heat source located at the top and bottom of the droplet), as shown in **FIGURE 5**. This figure is the illustration of a representative case taken from a 30 experiments samples. It is evident that the emulsion with the larger mean diameter is more prone to coalescence than the finer one. The micro-explosion rate is the higher in the configuration A (80%), while it decreases to 50% in the configuration B. The fine emulsion (configuration C and D) never ended up in micro-explosion. A total of 30 cases are studied in each configuration to reduce errors due to the stochastic behavior of micro-explosion. All the results are summed-up in**TABLE 2**. It clearly shows that coalescence promotes micro-explosion rate, due to the higher quantity of energy accumulated in a big water droplet with respect to a single smaller droplet.

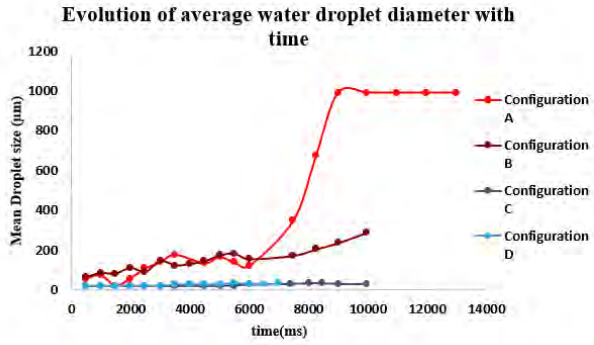

Figure 5. Coalescence rate of water subdroplets during heating phase

FIGURE 6 shows the difference in pattern between a coarse and fine emulsion during heating with the radiative source coming from the bottom of the droplet. Both compared frames have been taken at the same time. It clearly shows, that, in the case of coarse emulsion, coalescence is fast and ends up in a single water droplet at the bottom of the mother drop, while for finer emulsion, convective motion of water droplets with lower coalescence rate is observed. The stronger internal convective motion observed in the fine sized emulsion can limitate the coalescence process and so way micro-

Configu ration	ME Rate	ME delay (Average) s)	ME delay Range [Min-Max]
A	80	16.4	[7.7-27.1]
B	50	18.3	[9.9-25.8]
C	0	N.A	N.A
D	0	N.A	N.A

Table 2. Results of Micro-Explosion rate and delay for the 4 configurations under study

explosion rate. . Deeper investigation on this internal motion of water droplets will be investigated by Particle-Tracking-Velocimetry. Micro-explosion de-

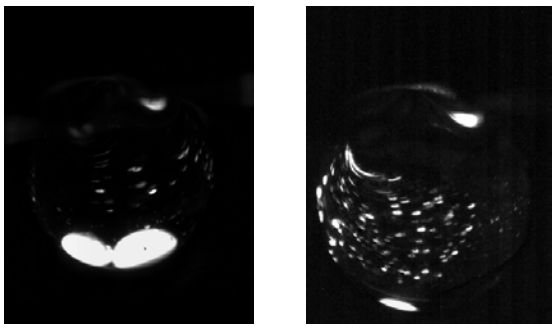

(a) (b)

Figure 6. Water droplets observation for coarse emulsion (a) and fine emulsion (b) during heating with bottom panel

lay was measured for different temperatures of the heating source for the A and B configurations. The main comparison is performed for the bottom panel at a temperature of 430°C and the top panel at a temperature of 700°C, since in both cases the total heat flux coming at the droplet is similar. The **FIGURE 7** plots micro-explosion delay as a function of temperature. As we can see, micro-explosion delays decreases while increasing temperature with the bottom panel configuration, which shows expected behavior. Top panel configuration at T=700°C and Bottom panel configuration at T=430°C have a similar range of micro-explosion delay,even if the heating processes involved are different(in the bottom panel case there is a part of the heat flux coming from natural convection which is not present in the top case being the droplet heating due to only radiative and conductive processes). Moreover, we can see that there is a large span of values for the delays which can be explained by the fact that micro-explosion is a stochastic process and its occurence delay can be reduced by fast nucleation at the wires locations, while it is increased when high metastable state occurs. This point will be investigated more deeply in an upcoming experiment by using 2 colors LIF for temperature measurements.

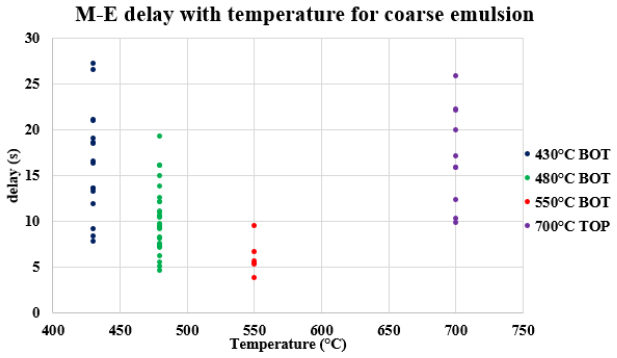

Figure 7. Micro-explosion delay at different temperatures and heating source location

Simplified Heating Model of Emulsion Droplet

A first simple model of an emulsion droplet has been considered in order to obtain insights on the behavior of the emulsion under radiant heating and to quantify the contribution of the different fluxes on the heating of the emulsion. In this simplified model, we considered only one droplet of water placed in the center of the emulsion mother drop, thus the interactions between fine dispersed water droplets are not taken into account. The continous phase used for the calculations was n-octane -that is an alkane hydocarbon as n-tetradecane- due to the abundance of information on its optical properties in the literature, even if its radiative properties can present some differences from n-tetradecane. The further approximation applied in the simplified model concerns the methodology utilized in the radiative calculations. It is typically used for bulks liquids or solids, while in this study, the object of interest is a droplet.

In order to compute the radiative power absorbed by the emulsion droplet, the first step is to calculate the absorptivity of the two fluids in the considered range of radiations [3-12 µm]. Absorptivity of semi-transparent material is given by the following equations :

$$A = 1 - \rho\left(1 + \frac{(1-\rho)^2\tau^2}{1-\rho^2\tau^2}\right) - \frac{(1-\rho)^2\tau}{1-\rho^2\tau^2} \quad (1a)$$

$$\tau = e^{-\kappa d} \quad (1b)$$

$$\rho = \frac{(n-1)^2 + k^2}{(n+1)^2 + k^2} \quad (1c)$$

Equation **(1a)** gives the absorptivity of the material, where τ is the transmission coefficient, given by the equation **(1b)** (with κ the absorption coefficient and d the thickness), and ρ the reflection coefficient, given by the equation **(1c)** (where n and k are the real and imaginary part of refractive index). As stated earlier, the parameters n, k and the absorption coefficient are taken from octane for the continuous phase. Once the two fluids are characterized in terms of macroscopic optical properties, the next step is to calculate the incident flux coming at the emulsion mother drop. **FIGURE 8** is a modelization of the simplified model we used for radiative flux calculation.

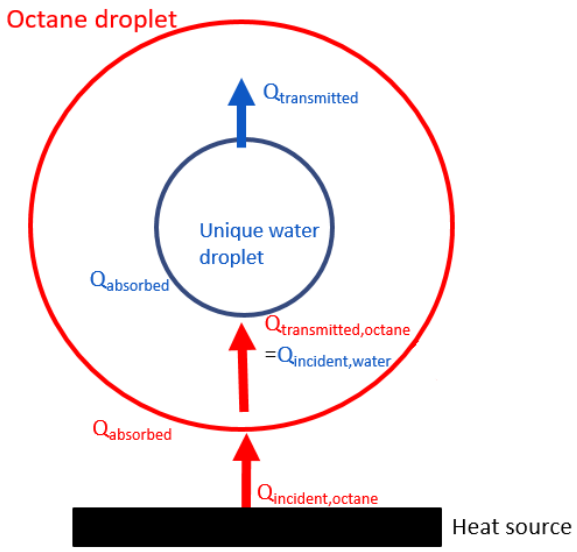

Figure 8. Scheme of the simplified model

The incident flux coming to the emulsion droplet is calculated as follow :

$$Q_{incident,octane} = F_{12}\epsilon\sigma S T_{panel}^4 \quad (2)$$

Where F_{12} is the view factor between the panel and the droplet (F_{12} =0.027), ϵ,S and T the emissivity, surface and temperature of the panel and σ the Stefan-Boltzmann constant.
Next we calculate the part of the incident flux absorbed and transmitted by the octane droplet. The part of the flux transmitted is then used as the incident flux for the water subdroplet since it is embedded inside of the emulsion mother droplet. Thus we have :

$$Q_{incident,water} = Q_{tansmitted,octane} \quad (3)$$

Where $Q_{incident,water}$ is the incident flux coming at the water droplet and $Q_{tansmitted,octane}$ is the transmitted flux by the octane droplet.

Once the incident flux coming at the unique water droplet is obtained, we then calculate the part of this incident flux absorbed, with the absorptivity of the water droplet calculated with equations set **Eq.1**. The **FIGURE 9** represents the spectral power absorbed by one droplet of water and octane in the wavelength-band of the heating panel.
The power absorbed by the oily-phase has also been calculated.

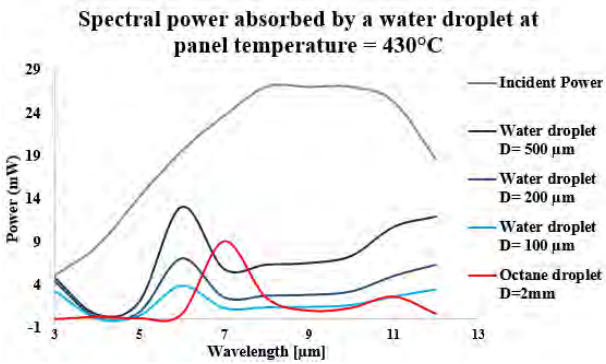

Figure 9. Spectral power absorbed by one octane and water droplet of different sizes

The different fluxes at the droplet have been compared with simplified models in order to have a first insight at which phenomenon is dominant :

$$Q_{cond} = \frac{\lambda_{air} S(T_{panel} - T_s)}{t_{air}} \quad (4a)$$

$$Q_{conv} = hS(T_{panel} - T_{air}) \quad (4b)$$

$$Q_{rad} = \int_{\lambda 1}^{\lambda 2} Q_{abs,water,\lambda} d\lambda + \int_{\lambda 1}^{\lambda 2} Q_{abs,octane,\lambda} d\lambda \quad (4c)$$

Equation **(4a)** represents the conductive flux between the panel and the droplet. In this case, we suppose that the air is immobile. Equation **(4b)** represents the model for the convective heat flux. We supposed that the convection coefficient h was

equal to 10 $Wm^{-2}K^{-1}$, which is a standard value in natural convection for air. For the radiant heat flux, equation **(4c)** is the sum of the spectral flux absorbed by one droplet of octane and one droplet of water for each wavelength of the emission spectrum. These equations are a very simplified model with respect to the real experiment to describe the different flux. In addition, it supposes that the heat fluxes are not time dependent.

FIGURE 10 shows the comparison between the conductive, convective and radiant heat flux at the droplet emulsion in the top and bottom panel configuration. In the bottom panel, we can observe that the droplet would be heated by both convection and radiation while, for the top configuration, the dominant heat flux is the radiant one. In fact, in the second case, there is no heating convective flow coming at the droplet, since the hot point is located over it. In the model we have considered stagnant air and this assumption generates the contribution due to conduction in the top heating configuration. However, this is correct in the first heating phase of the radiant panel. After, as the panel heats up, the rising current of hot air it generates will cause an upward motion of cold air from below and, therefore, the conductive contribution can be reduced or cancel out.

The differences in the radiant heat flux between the top panel and the bottom panel configuration comes from the panel temperature, which has been set to 430°C for the bottom case and 700°C in the top case in order to provide the same overall droplet heating (see **FIGURE 4**).

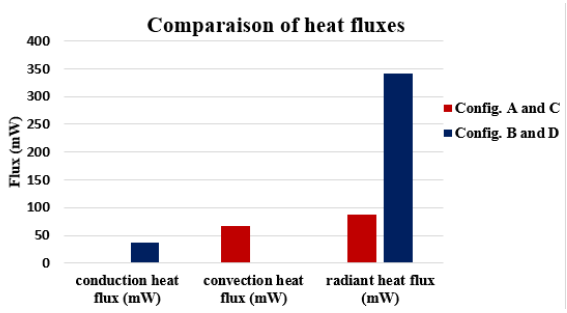

Figure 10. Comparison of heat fluxes coming at the emulsion droplet (water + oil)

Even if the computation reported in **FIGURE 10** have been performed a simplified model with respect to the real experiment, they allow us to analyse a peculiar phenomenology was noticed. Indeed it, was qualitatively observed convective motion of the water embedded droplets inside the emulsion mother droplet, **even when the heating source was located at the top of the droplet**.The calculation showed that the heat flux was mainly radiative for the heat source located at the top while it was both convective and radiative for the heat flux located at the bottom. Thus, in the case of the top panel heating, it would mean that, since the hot point is located at the top of the emulsion drop, the convective motion should not happen.

However, two additional effects have to be considered. One is the ascensional motion of the air from the bottom generated by the hot panel placed on the top. This upward motion of cold air generates a shear stress on the droplet surface that can be responsible of liquid motion inside the droplet. However, considering the relatively low Reynold number, this effect should be very limited.

The second effect is due to the lensing power of a droplet. Indeed, the curved surface of a droplet acts like a convergent lens with respect to the radiation hitting on it. Depending on the curvature (droplet diameter) and refractive index (i.e., temperature and composition of the droplet and radiation wavelength), the radiation can be focused in a region inside or outside the droplet placed in the opposition side with respect to the direction of the incoming radiation. In the specific case, being the radiative panel placed on the top, the radiation is focused in a zone localised in the bottom region. The presence of a focal point or, in any case, higher density of radiation in the bottom side of the droplet, will generate in that region a hotter zone that contributes to generate liquid internal motion. In the bottom configuration, the radiative source is located below the droplet and calculation showed that the heat flux is both convective and radiative. Similarly, to the discussion above, the lensing effect of the droplet can produce a concentration of radiation, inside or outside the droplet, which will be localised in the top region for radiation coming from the bottom.

However, as discussed in **FIGURE 10**, due to the lower temperature of the bottom panel, 430°C with respect to 700°C in the top configuration, the radiative flow on the droplet is reduced significantly. Thus, this effect is less relevant in the bottom configuration and the main hotter region of the droplet is the lower one due to the hot convective flow from the bottom.

The occurring of the lensing effect in case of an emulsion droplet deserve a specific study. Indeed, the great number of primary droplets forming

the disperse phase typically generates multiple scattering. This, homogenizing the diffusion of radiation inside the emulsion droplet, destroys the lensing effect and the droplet appears opalescent. The multiple scattering depends on the size and number concentration of the dispersed phase and, hence, the process is time-dependent as consequence of the coalescence process of water droplets in the emulsion.

A specific study is also required to take into account the heat exchange between the emulsion droplet and the crossed wires used for its suspension. Such wires are exposed to radiative, convective and conductive heat flows and establish a heat bridge between the droplet and the external ambient. Depending on the thermal conditions, the wires can conduct heat inside the suspended droplet or act as a heat sink subtracting heat from the droplet.

First insights on internal motion of water subdroplets

The presented experiment shows an important difference of behavior between coarse and fine emulsions. In the case of fine emulsions, strong internal motion of water droplets is observed, due to natural convection. The Laser Induced Fluorescence technique was applied to fine emulsion droplets perform Particle Tracking Velocimetry (PTV) analysis of the water droplets motion [21]. The frames recorded were post-processed and their center position (x and y coordinates) and radius were measured. Since the visibility of the water droplets within the emulsion mother drop is not of constant quality during the full experiment, only some sequences were analysed with PTV. This change in visibility of the water subdroplets can be explained mainly by two factors :

1. The analysis of the movies permits to note that, just after the injection, the emulsion droplets are opalescent. The "milky" aspect is due to the multiple scattering generated by the high number concentration of water subdroplets of small size. Few seconds after the heating start, the emulsion droplets become transparent. This change can be explained by considering that during this phase water subdroplets gather, partially coalesce and evaporate, thus reducing drastically their concentration. As a result, the water inter-droplets distance overcomes the single scattering limit and a transition from multiple scattering to single scattering regime occurs, thus making the emulsion droplets transparent. In addition, the fluorescence signal of the Fluorescein Sodium Salt increases with temperature, which means that the signal quality increases with time.
2. The emulsion droplet is cut vertically by the laser sheet. Nevertheless, the convective motion of the droplets happens in a 3 dimensional space, which means that from one frame to another, water droplets can move out of the visualization plan. However, identifications of trajectories were possible. For each PTV analysis, 200 frames were taken into account (corresponding to a duration of 200 ms).

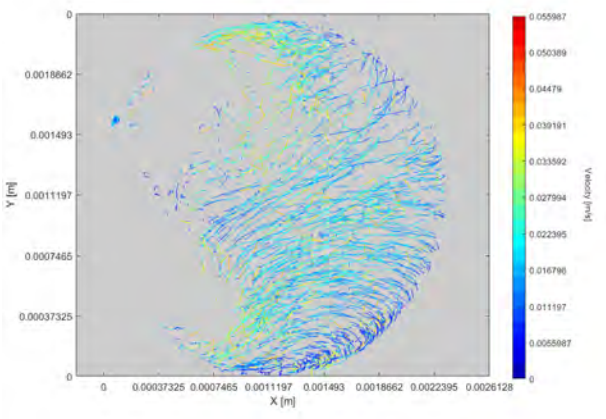

Figure 11. Example of trajectories of water subdroplets in a 200 ms frame with top panel heating

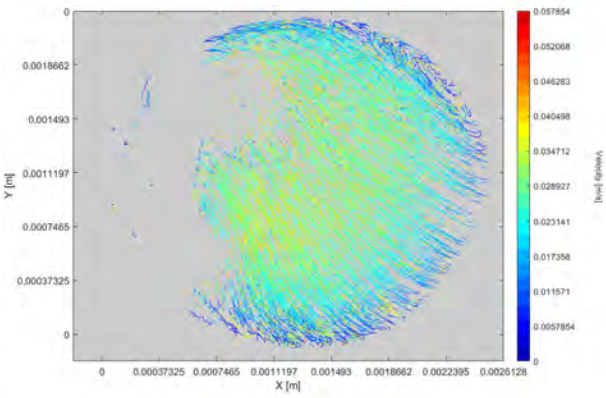

Figure 12. Example of trajectories of water subdroplets in a 200 ms frame with bottom panel heating

FIGURES 11 and 12 show plots of trajectories of water subdroplets heated by the top and bottom panel respectively. The results are very different in terms of both trajectories and intensity

(i.e., velocity values). For the top case, we observe two main streamlines within the droplet, but with a low intensity in terms of velocity. One stream line consists of a low circular motion in the range Y = [0-0.7465] mm. Then, on the upper part of the drop, we can distinguish an upward motion with low intensity. For the bottom case, there is a more uniform velocity field. First, the values of the velocities are higher with respect to the top case heating. Thus, we can see this global motion, going from the upper left part of the mother drop, down to the lower right part of the mother drop. In a 3 dimensional space, it would result in a toroidal motion of the water subdroplets, with a small angle of deviation with respect to the vertical axis. This global transportation of the water subdroplets in the same directions will inhibit the merging and coalescence, thus micro-explosion probability.
The difference in the velocity fields bewteen the top and bottom panel case can be explained by the way that the droplet is heated. In the top case, as stated earlier, the droplet is heated mainly by radiative heating, and the focusing effect of the emulsion droplets tends to create a hot point located in the lower region of the droplet. In the bottom case, the heat flux is also convective, which results in a bigger area heated (all the bottom of the droplet is heated with respect to one local point in the other case) which results in a more global convective motion with an important vertical component. Further investigations are required in order to understand deeper the focusing of incident radiations by the mother drop. The effect of the illuminating laser (altough its power was fixed at the minimum value of 0.5 W) is still a remaining question.

For the coarse emulsion cases, almost no natural convection is observed, making impossible the use of PTV processing. Emulsion droplet undergo fast sedimentation and coalescence, with high micro-explosion rate.

Conclusion

In this paper, the influence of the dispersed phase size and motion under radiant heating on micro-explosion efficiency has been studied. The following points have been investigated :

1. The Laser Induced Fluorescence technique makes possible the observation of the dispersed water subdroplets during the heating of the emulsion. Evolution of size with time can be studied. First results of Particle Tracking Velocimetry algorithms showed that the LIF can also be used in order to track subdroplets position and velocity.
2. The dispersion of the emulsion plays a first plan role on micro-explosion rate. Coarse emulsion (D_{moy} =20 μm) shows micro-explosion rate of 80% and 50% under bottom and top location radiant heating respectively, while for finer emulsion (D_{moy} =12 μm), micro-explosion never happens.
3. Water subdroplets motion caused by natural convection has been observed for the finer emulsion. This convective motion tends to be a limitant factor for micro-explosion since coalescence is reduced by convection movements. High coalescence rate happens indeed when the water droplets are located in the same region of the mother droplet (at the bottom due to sedimentation).
4. The focusing lens effect of the droplet induces a hotter region in the opposite side with respect to the incoming flow direction. This effect is more significant in the top configuration due to the high heating temperature and it can contribute to generate internal movements of the water subdroplets.

Next septs of the work will aim to provide a deeper understanding on the mechanism of radiant heating of emulsion, where the two phases do not have the same optical properties. Radiative properties of n-tetradecane in the infrared band will be investigated, in order to obtain more precise informations on the refractive index. The presented model will be refined. Two colors LIF method will be used in order to obtain temperature field, both within the oily and water phase.

Nomenclature

A	absorptivity
F_{12}	view factor panel/droplet
h	convection coefficient
k	imaginary part of the refractive index
n	real part of the refractive index
Q_{cond}	conductive flux
Q_{conv}	convective flux
$Q_{incident,octane}$	Incident radiative flux at the octane droplet
$Q_{incident,water}$	Incident radiative flux at the water droplet
Q_{rad}	radiative flux
S	surface
T_{air}	Ambiant air temperature
T_{panel}	panel temperature

Greek

λ	wavelength
ρ	reflexion coefficient
τ	transmission coefficient
κ	absorption coefficient
σ	Stephan Boltzmann constant
ϵ	emissivity
λ_{air}	air thermal conductivity

References

[1] J.W. Park and K.Y. Huh andJ.H. Lee. *Journal of Automobile Engineering*, 215:83–93, 2001.

[2] O. Armas, R. Ballesteros, F.J. Martos, and J.R. Agudelo. *Fuel*, 84:1011–1018, 2005.

[3] M. Abdollahi, B. Ghobadian, G. Najafi, S.S. Hoseiniand, M.Mofijurand, and M. Mazlan. *Fuel*, 280, 2020.

[4] R.S.Volkov and P.A.Strizhak. *Internal Journal of Thermal Sciences*, 127:126–141, 2018.

[5] E. Mura, C. Josset, K. Loubar, G. Huchet, and J. Bellettre. *Atomization and Sprays*, 20:791–799, 2010.

[6] D. Antonov, M. Piskunov, P. Strizhak, D. Tarlet, and J. Bellettre. *Fuel*, 259, 2020.

[7] M.Y. Khan, Z.A. Abdul Karim andA.R.A. Aziz, and I.M. Tan. *Energy Fuels*, 28, 2014.

[8] H. Watanabe, Y. Suzuki, T. Harada, Y. Matsushita . Aoki, and T. Miura. *Energy*, 35:806–813, 2010.

[9] V. Califano, R. Calabria, and P. Massoli. *Fuel*, 2014.

[10] E.A. Melo-Espinosa, J. Bellettre, D. Tarlet, A. Montillet, R. Piloto-Rodríguez, and S. Verhelst. *Fuel*, 219, 2018.

[11] H. Watanabe, T. Harada, Y. Matsushita, H. Aoki, and T. Miura. *International Journal of Heat and Mass Transfer*, 52:3676–3684, 2009.

[12] O. Moussa, D.Tarlet, P. Massoli, and J. Bellettre. *International Journal of Thermal Sciences*, 133:90–97, 2018.

[13] D. Tarlet, C. Josset, and J. Bellettre. *International Journal of Heat and Mass Transfer*, 95:689–692, 2016.

[14] Y. Suzuki, T. Harada, H. Watanabe, M. Shoji, Y. Matsushita, H. Aoki, and T. Miura. *Proceedings of the Combustion Institute*, 33:2063–2070, 2011.

[15] D.V. Antonov, M.V. Piskunov, and P.A. Strizhak. *Applied Thermal Engineering*, 152, 2019.

[16] O. Moussa, D. Tarlet, P. Massoli, and J. Bellettre. *Experimental Thermal and Fluid Science*, 116, 2020.

[17] L.A. Torres, B.A. Fleck, D.J. Wilson, and D.S. Nobes. *Measurement*, 46:2597–2607, 2013.

[18] P.A. Strizhak, R.S. Volkov, O. Moussa, D. Tarlet, and J. Bellettre. *International Journal of heat and Mass transfer*, 163, 2020.

[19] S.M Syed Masharuddin, Z.A.A Karim, M.A Meor ans S.N.Amran, and M. A.Ismael. *Alexandria Engineering Journal*, pp. 541–547, 2021.

[20] P.V. Bulat, K.N. Volkov, and E. Ye. Ilyina. *International Electronic Journal of Mathematics Education*, 11:3009–3020, 2016.

[21] D. Tarlet, C. Bendicks, C. Roloff, R. Bordás, B. Wunderlich, B. Michaelis, and D. Thévenin. *Flow, Turbulence and Combustion*, 88, 2012.